













# Overdominant Effect of a *CHRNA4* Polymorphism on Cingulo-Opercular Network Activity and Cognitive Control

 Sepideh Sadaghiani,<sup>1,2,3</sup>  Bernard Ng,<sup>1,4</sup> Andre Altmann,<sup>1,5</sup> Jean-Baptiste Poline,<sup>6</sup> Tobias Banaschewski,<sup>7</sup>  Arun L.W. Bokde,<sup>8</sup> Uli Bromberg,<sup>9</sup> Christian Büchel,<sup>9</sup> Erin Burke Quinlan,<sup>10</sup> Patricia Conrod,<sup>10</sup> Sylvane Desrivieres,<sup>10</sup>  Herta Flor,<sup>11,12</sup> Vincent Frouin,<sup>13</sup> Hugh Garavan,<sup>14</sup>  Penny Gowland,<sup>15</sup> Jürgen Gallinat,<sup>16</sup>  Andreas Heinz,<sup>16</sup> Bernd Ittermann,<sup>17</sup>  Jean-Luc Martinot,<sup>18,19,20,21</sup> Marie-Laure Paillère Martinot,<sup>19,22</sup>  Hervé Lemaitre,<sup>18</sup> Frauke Nees,<sup>7,11</sup>  Dimitri Papadopoulos Orfanos,<sup>13</sup> Tomáš Paus,<sup>23</sup> Luise Poustka,<sup>24,25</sup>  Sabina Millenet,<sup>7</sup> Juliane H. Fröhner,<sup>26</sup> Michael N. Smolka,<sup>26</sup> Henrik Walter,<sup>16</sup>  Robert Whelan,<sup>27</sup> Gunter Schumann,<sup>10</sup>  Valerio Napolioni,<sup>1</sup> and Michael Greicius<sup>1</sup>

<sup>1</sup>Department of Neurology and Neurological Sciences, Stanford University, Stanford, California 94305, <sup>2</sup>Department of Psychology, University of Illinois at Urbana-Champaign, Urbana, Illinois 61801, <sup>3</sup>Beckman Institute for Advanced Science and Technology, Urbana, Illinois 61801, <sup>4</sup>Department of Statistics, University of British Columbia, Vancouver BC V6T 1Z4, Canada, <sup>5</sup>Translational Imaging Group, Centre for Medical Image Computing, Department of Medical Physics and Bioengineering, University College London, London WC1E 6BT, United Kingdom, <sup>6</sup>Department of Psychology, University of California, Berkeley, California 94720, <sup>7</sup>Department of Child and Adolescent Psychiatry and Psychotherapy, Central Institute of Mental Health, Medical Faculty Mannheim, Heidelberg University, 68159 Mannheim, Germany, <sup>8</sup>Discipline of Psychiatry, School of Medicine and Trinity College Institute of Neuroscience, Trinity College, Dublin 2, Ireland, <sup>9</sup>University Medical Centre Hamburg-Eppendorf, 20246 Hamburg, Germany, <sup>10</sup>Medical Research Council, Social, Genetic and Developmental Psychiatry Centre, Institute of Psychiatry, Psychology and Neuroscience, King's College London WC2R 2LS, United Kingdom, <sup>11</sup>Department of Cognitive and Clinical Neuroscience, Central Institute of Mental Health, Medical Faculty Mannheim, Heidelberg University, 68159 Mannheim, Germany, <sup>12</sup>Department of Psychology, School of Social Sciences, University of Mannheim, 68131 Mannheim, Germany, <sup>13</sup>NeuroSpin, CEA, Université Paris-Saclay, F-91191 Gif-sur-Yvette, France, <sup>14</sup>Departments of Psychiatry and Psychology, University of Vermont, Burlington, Vermont 05405, <sup>15</sup>Sir Peter Mansfield Imaging Centre School of Physics and Astronomy, University of Nottingham, University Park, Nottingham NG7 2RD, United Kingdom, <sup>16</sup>Department of Psychiatry and Psychotherapy, Campus Charité Mitte, Charité, Universitätsmedizin Berlin, 10117 Berlin, Germany, <sup>17</sup>Physikalisch-Technische Bundesanstalt, 10587 Berlin, Germany, <sup>18</sup>Institut National de la Santé et de la Recherche Médicale, INSERM Unit 1000 “Neuroimaging & Psychiatry”, University Paris Sud – Paris Saclay, 91400 Orsay, France, <sup>19</sup>University Paris Descartes, 75006 Paris, France, <sup>20</sup>Service Hospitalier Frédéric Joliot, 91400 Orsay, France, <sup>21</sup>Maison de Solenn, Cochin Hospital, 75014 Paris, France, <sup>22</sup>AP-HP, Department of Adolescent Psychopathology and Medicine, Maison de Solenn, Cochin Hospital, 75014 Paris, France, <sup>23</sup>Rotman Research Institute, Baycrest and Departments of Psychology and Psychiatry, University of Toronto, Toronto, Ontario M6A 2E1, Canada, <sup>24</sup>Department of Child and Adolescent Psychiatry and Psychotherapy, University Medical Centre Göttingen, 37075 Göttingen, Germany, <sup>25</sup>Clinic for Child and Adolescent Psychiatry, Medical University of Vienna, 1090 Vienna, Austria, <sup>26</sup>Department of Psychiatry and Neuroimaging Center, Technische Universität Dresden, 01069 Dresden, Germany, and <sup>27</sup>School of Psychology and Global Brain Health Institute, Trinity College Dublin 2, Ireland

The nicotinic system plays an important role in cognitive control and is implicated in several neuropsychiatric conditions. However, the contributions of genetic variability in this system to individuals' cognitive control abilities are poorly understood and the brain processes that mediate such genetic contributions remain largely unidentified. In this first large-scale neuroimaging genetics study of the human nicotinic receptor system (two cohorts, males and females, fMRI total  $N = 1586$ , behavioral total  $N = 3650$ ), we investigated a common polymorphism of the high-affinity nicotinic receptor  $\alpha4\beta2$  (rs1044396 on the *CHRNA4* gene) previously implicated in behavioral and nicotine-related studies (albeit with inconsistent major/minor allele impacts). Based on our prior neuroimaging findings, we expected this polymorphism to affect neural activity in the cingulo-opercular (CO) network involved in core cognitive control processes including maintenance of alertness. Consistent across the cohorts, all cortical areas of the CO network showed higher activity in heterozygotes compared with both types of homozygotes during cognitive engagement. This inverted U-shaped relation reflects an overdominant effect; that is, allelic interaction (cumulative evidence  $p = 1.33 \times 10^{-5}$ ). Furthermore, heterozygotes performed more accurately in behavioral tasks that primarily depend on sustained alertness. No effects were observed for haplotypes of the surrounding *CHRNA4* region, supporting a true overdominant effect at rs1044396. As a possible mechanism, we observed that this polymorphism is an expression quantitative trait locus modulating *CHRNA4* expression levels. This is the first report of overdominance in the nicotinic system. These findings connect *CHRNA4* genotype, CO network activation, and sustained alertness, providing insights into how genetics shapes individuals' cognitive control abilities.

**Key words:** alertness; cingulo-opercular network; fMRI; genetics; nicotinic acetylcholine receptor; polymorphism

## Significance Statement

The nicotinic acetylcholine system plays a central role in neuromodulatory regulation of cognitive control processes and is dysregulated in several neuropsychiatric disorders. Despite this functional importance, no large-scale neuroimaging genetics studies have targeted the contributions of genetic variability in this system to human brain activity. Here, we show the impact of a common polymorphism of the high-affinity nicotinic receptor  $\alpha4\beta2$  that is consistent across brain activity and behavior in two large human cohorts. We report a hitherto unknown overdominant effect (allelic interaction) at this locus, where the heterozygotes show higher activity in the cingulo-opercular network underlying alertness maintenance and higher behavioral alertness performance than both homozygous groups. This gene–brain–behavior relationship informs about the biological basis of inter-individual differences in cognitive control.

## Introduction

Cognitive control abilities are central to all goal-directed behavior but vary widely across individuals (Gruszka et al., 2010; Mennes et al., 2011). Although cognitive control capacities have strong heritable components (Friedman et al., 2008; Chang et al., 2013), it is largely unknown through which brain mechanisms genetic variability translates into their interindividual differences. Neuromodulatory neurotransmitter systems are central to cognitive control given their capacity to modify signal processing broadly across large areas of the brain. In particular, the broad acetylcholinergic innervation of the neocortex originating in the basal forebrain plays a central role in cognitive control, especially tonic control functions (Knott et al., 1999; Kozak et al., 2006). Both tonic control functions and acetylcholinergic modulation are dysregulated in several neuropsychiatric disorders (Lesh et al.,

2011; Sarter and Paolone, 2011; Higley and Picciotto, 2014), reward processing, and addiction to various substances (Hendrickson et al., 2013). However, how genetic polymorphisms in this modulatory system influence brain function is poorly understood.

The most abundant high-affinity nAChR in the mammalian brain is the  $\alpha4\beta2$  receptor (Albuquerque et al., 2009). Among the single nucleotide polymorphisms (SNPs) of the underlying genes *CHRNA4* and *CHRNA2*, rs1044396 (NM\_000744.6:c.1629C>T) of the  $\alpha4$  subunit (chromosome 20q13.3) has been implicated in behaviorally relevant contexts, albeit with inconsistent impact from major/minor alleles. Although this SNP itself is synonymous (NP\_000735.1:p.Ser543=), it is part of a functional *CHRNA4* haplotype affecting receptor sensitivity to acetylcholine (Eggert et al., 2015). The SNP is implicated in nicotine consumption and addiction (Feng et al., 2004; Breitling et al., 2009), as well as phasic cognitive control functions. However, this cognitive literature (often comprising relatively small sample sizes) is inconclusive because some studies report a behavioral advantage of the rs1044396-T allele (Espeseth et al., 2010; Greenwood et al., 2012, 2005) and some the rs1044396-C allele (Parasuraman et al., 2005; Reinvang et al., 2009). Furthermore, the brain mechanisms mediating the impact on behavior are largely unknown. The only two neuroimaging investigations of rs1044396 have been performed in relatively small sample sizes  $N < 50$  and one study lacks heterozygous participants (Winterer et al., 2007; Giessing et al., 2012).

The cortical target regions of acetylcholinergic stimulation may shed light on the underlying pathway from genetic variability to cognitive abilities. Using positron emission tomography, we found that, across the cerebral cortex,  $\alpha4\beta2$  receptor density was highest bilaterally in the dorsal anterior cingulate cortex and anterior insula (Picard et al., 2013). Together with the thalamus, the brain region with the highest nAChR density (Gallezot et al., 2005), these areas constitute the core of the cingulo-opercular (CO) network, also referred to as salience network (see Fig. 2A) (Dosenbach et al., 2006; Seeley et al., 2007). The anatomically selective mapping of  $\alpha4\beta2$  receptor density to this network generates a targeted hypothesis regarding the brain structures mediating the cognitive impact of the  $\alpha4$  polymorphism rs1044396.

The spatial relation between the CO network and  $\alpha4\beta2$  nAChR density suggests that functional differences in this receptor may affect the cognitive function of the CO network. Several lines of research suggest that one core cognitive control function of the CO network is the maintenance of sustained/tonic alertness or vigilance (Sturm et al., 2004; Sadaghiani et al., 2010). Tonic alertness describes the mentally effortful, self-initiated (rather than externally driven), and continuous preparedness to process information and to respond (Parasuraman, 1998; Posner, 2008). A

Received April 12, 2017; revised Aug. 20, 2017; accepted Aug. 22, 2017.

Author contributions: S.S., A.A., V.N., and M.G. designed research; S.S., B.N., A.A., and V.N. performed research; S.S., B.N., A.A., J.-B.P., T.B., A.B., U.B., C.B., E.B.O., P.C., S.D., H.F., V.F., H.G., P.G., J.G., A.H., B.I., J.-L.M., M.-L.P.M., H.L., F.N., D.P.O., T.P., L.P., S.M., J.F., M.N.S., H.W., R.W., and G.S. contributed unpublished reagents/analytic tools; S.S., B.N., A.A., and V.N. analyzed data; S.S., V.N., and M.G. wrote the paper.

We thank all investigators contributing to the Philadelphia Neurodevelopmental Cohort, especially Theodore D. Satterthwaite, for supporting this work. We thank Stephen M. Malone for supporting us in a multimodal investigation of *CHRNA4*. This work was supported by funding from The Feldman Family Foundation; the J.W. Bagley Foundation; the Medical Research Council (MRC grant MR/L016311/1). The IMAGEN consortium has received support from the following sources: the European Union-funded FP6 Integrated Project IMAGEN (Reinforcement-related behaviour in normal brain function and psychopathology; LSHM-CT-2007-037286), the Horizon 2020 funded European Research Council Advanced Grant STRATIFY (Brain network based stratification of reinforcement-related disorders; 695313), ERANID (Understanding the Interplay between Cultural, Biological and Subjective Factors in Drug Use Pathways; PR-ST-0416-10004), BRIDGET (JPND: BBrain Imaging, cognition Dementia and next generation GEnomics; MR/N027558/1), the FP7 projects IMAGEMEND(602450; IMAGING GEnetics for MEntal Disorders) and MATRICS (603016), the Innovative Medicine Initiative Project EU-AIMS (115300-2), the Medical Research Council Grant c-VEDA (Consortium on Vulnerability to Externalizing Disorders and Addictions; MR/N000390/1), the Swedish Research Council FORMAS, the Medical Research Council, the National Institute for Health Research (NIHR) Biomedical Research Centre at South London and Maudsley NHS Foundation Trust and King's College London, the Bundesministerium für Bildung und Forschung (BMBF Grants 01GS08152; 01EV0711; eMed SysAlc01ZX1311A; Forschungsnetz AERIAL), the Deutsche Forschungsgemeinschaft (DFG Grants SM 80/7-1, SM 80/7-2, SFB 940/1). Further support was provided by grants from: Agence Nationale de la Recherche (ANDR project AF12-NEURO008-01-WM2NA, and ANR-12-SAMA-0004), the Fondation de France, the Fondation pour la Recherche Médicale, the Mission Interministérielle de Lutte-contre-les-Drogues-et-les-Conduites-Addictives (MILDECA), the Assistance-Publique-Hôpitaux-de-Paris and Institut National de la Santé et de la Recherche Médicale (INSERM interface grant), Paris Sud University IDEX 2012; the National Institutes of Health (NIH), Science Foundation Ireland (16/ERC/D/3797; Axon, Testosterone and Mental Health during Adolescence; Grant R01 MH085772-01A1), and by NIH Consortium (Grant U54 EB020403), supported by a cross-NIH alliance that funds Big Data to Knowledge Centres of Excellence. A.A. holds an MRC eMedLab Medical Bioinformatics Career Development Fellowship.

T.B. has served as an advisor or consultant to Bristol-Myers Squibb, Desitin Arzneimittel, Eli Lilly, Medice, Novartis, Pfizer, Shire, UCB, and Vifor Pharma; he has received conference attendance support, conference support, or speaking fees from Eli Lilly, Janssen McNeil, Medice, Novartis, Shire, and UCB; and he is involved in clinical trials conducted by Eli Lilly, Novartis, and Shire; the present work is unrelated to these relationships. H.W. received a speaker honorarium from Servier (2014). The remaining authors declare no competing financial interests.

Correspondence should be addressed to Sepideh Sadaghiani, Ph.D., Assistant Professor, Department of Psychology, Cognitive Neuroscience Division, Beckman Institute for Advanced Science and Technology, University of Illinois at Urbana-Champaign, Beckman Institute, 405 N Mathews Avenue, Urbana, IL 61801. E-mail: Sepideh@uiuc.edu.

DOI:10.1523/JNEUROSCI.0991-17.2017

Copyright © 2017 the authors 0270-6474/17/379658-10\$15.00/0

**Table 1. Demographics and genotype breakdown of included subjects**

	IMAGEN cohort		PNC cohort	
	fMRI	Behavioral	fMRI	Behavioral
T/T carriers	354 (189 females)	403 (209 females)	66 (37 females)	608 (333 females)
T/C carriers	671 (340 females)	751 (383 females)	111 (55 females)	1077 (573 females)
C/C carriers	333 (166 females)	345 (168 females)	51 (25 females)	466 (250 females)
Total	1358 (695 females)	1499 (760 females)	228 (117 females)	2151 (1156 females)
Age (y)	14 ± 0	14 ± 0	16.9 ± 1.8	16.7 ± 1.9

distinctive characteristic of the CO network is that it becomes active whenever cognitive engagement is required regardless of the specific task (Dosenbach et al., 2006; Yeo et al., 2015), likely due to tonic alertness demands present across cognitive tasks (Sadaghiani and D'Esposito, 2015).

Here, we test the hypothesis that the  $\alpha4\beta2$  nAChR genotype affects CO network activation during cognitively demanding tasks and explains performance differences in tonic alertness. We focus on the *CHRNA4* rs1044396 genotype in light of the above-described prior behavioral literature. We study the impact of this polymorphism on brain activity and behavior in a large dataset in adolescents, with replication in an independent cohort of adolescents and young adults.

## Materials and Methods

### Subjects

Adolescents and young adults of Caucasian descent were investigated in two cohorts, IMAGEN and Philadelphia Neurodevelopmental Cohort (PNC), as detailed in Table 1. The IMAGEN cohort contains >2000 subjects studied in eight cities across Europe. The cohort and data acquisition have been described in detail previously (Schumann et al., 2010). All subjects were 14 years of age at the time of data collection. We retained all subjects with SNP rs1044396 imputation accuracy >0.9 (see “Genetics” section below). Among these,  $n = 1499$  subjects had behavioral data in the rapid visual processing task and  $n = 1358$  subjects had neuroimaging data in the stop signal task (see “fMRI acquisition” section below). Pubertal development stage was determined for use as a covariate using the Puberty Development Scale (Petersen et al., 1988), a self-reported measure of physical development based on the scale introduced by Tanner (1978). On this five-category scale, the vast majority of subjects had a puberty category score of 3 or 4 (median [interquartile range] = 4[1]).

From >8000 American subjects studied in Philadelphia for the PNC cohort, all of those who identified as being of Caucasian descent (not including mixed ethnicities) were selected for ethnic homogeneity and comparability with the IMAGEN cohort ( $n = 4734$ ). The cohort and data acquisition were described in detail previously (Satterthwaite et al., 2014, 2016). We retained all subjects with SNP rs1044396 imputation accuracy >0.9. For comparability with the IMAGEN dataset, only subjects of at least 14 years of age were included (range 14–22). Among these,  $n = 2151$  had behavioral data in the Penn continuous performance test (CPT) experiment and  $n = 228$  had neuroimaging data in the  $n$ -back experiment.

### Genetics

IMAGEN subjects were genotyped from blood samples on 610-Quad SNP and 660-Quad SNP arrays from Illumina. The vast majority of PNC subjects were genotyped from blood samples on the 550HH and 610-Quad SNP arrays from Illumina. Because rs1044396 SNP was not included in the Illumina array platforms by the IMAGEN and PNC consortia, we imputed *CHRNA4* rs1044396 using the Haplotype Reference Consortium r1.1. as a reference panel (McCarthy, 2016). In the IMAGEN cohort, *CHRNA4* rs1044396 was successfully imputed for 89.3% of the subjects using the Sanger Imputation Service (<https://imputation.sanger.ac.uk/>) with EAGLE2 (Loh et al., 2016) and PBWT (Durbin, 2014); minor allele frequency (MAF) was 0.479, as expected in Caucasians (European 1000 Genomes Consortium Phase 3 MAF = 0.471; 1000 Genomes Project Consortium, 2015). In the PNC cohort, *CHRNA4* rs1044396 was successfully im-

puted for 88.4% of the subjects using the Michigan Imputation Server (<https://imputationserver.sph.umich.edu/>) (Das et al., 2016) with SHAPEIT2 (Delaneau et al., 2013) and Minimac3 (Das et al., 2016). Note that, although imputation was performed on different servers for the two cohorts, because this process was completed at different instances and sites, both servers used an identical reference set. The MAF was 0.472. Genotype distribution did not deviate from Hardy–Weinberg equilibrium in the IMAGEN ( $p = 0.77$ ) and PNC ( $p = 0.99$ ) cohorts.

Linkage disequilibrium (LD) analysis was performed using Haploview version 4.2 and defining LD blocks based on the solid spine of LD algorithm (Barrett et al., 2005). Haplotype-based association testing was performed using PLINK by logistic regression model, adjusting for the same covariates used in the analysis of individual datasets. Results from each dataset were fixed-effect meta-analyzed using GWAMA (Mägi and Morris, 2010).

### fMRI acquisition

At IMAGEN sites, structural and functional MRI was performed on 3 T scanners from a range of manufacturers (at Hamburg, Mannheim, Dresden, and Paris: Siemens Trio with 12-channel head coil, Siemens; at Berlin: Siemens Verio with 8- and 12-channel head coils; at Dublin and Nottingham: Philips Achieva with 8-channel head coil; and at London: GE HDx with 8-channel head coil). A set of imaging sequence parameters compatible with all scanners, particularly those directly affecting image contrast or signal-to-noise, was devised and held constant across sites. Functional imaging parameters consisted of 8 min echoplanar imaging with TR/TE/flip angle = 2200 ms/30 ms/75°,  $64 \times 64 \times 40$  voxels with 2.4 mm slice thickness and 1 mm slice gap and a field of view of  $218 \times 218$  mm, yielding isotropic 3.4 mm voxels. The structural image consists of a T1-weighted MPRAGE image of  $256 \times 256 \times 160/166$  voxels (depending on manufacturer) with a 1.1 mm isotropic voxel size. Details are provided in Schumann et al. (2010). Functional images in the PNC cohort were recorded on a Siemens TIM trio scanner with 32-channel head coil and consisted of 11.6 min echoplanar imaging with TR/TE/flip angle = 3000 ms/32 ms/90°,  $64 \times 64 \times 46$  voxels with 3 mm slice thickness and no slice gap and a field of view of  $192 \times 192$  mm, yielding isotropic 3 mm voxels. The structural image consists of a T1-weighted MPRAGE image of  $192 \times 256 \times 160$  voxels, with a  $0.9 \times 0.9 \times 1$  mm voxel size. Details have been described previously (Satterthwaite et al., 2013, 2014).

### Experimental design

**Tasks for fMRI.** Both the IMAGEN and PNC datasets included neuroimaging during tasks demanding high cognitive engagement. In the IMAGEN dataset, among four fMRI runs (a functional localizer and three other tasks), we chose to investigate the stop signal task due to its high cognitive control demands. This task requires subjects to press a left or a right button in response to regularly presented visual “go” stimuli (left- or right-pointing arrows, respectively, every 1.6 to 2 s), but to withhold response if the go stimulus was followed by a “stop” signal (upward-pointing arrow). The stop signal was presented unpredictably across trials and the time between the foregone go stimulus and the stop signal (stop signal delay) was adjusted continuously during the run so as to keep the individual subject's stop success at 50%. Stop signal delay (range 0–900 ms) was increased or decreased from an initial duration of 150 ms at the beginning of the experiment in steps of 50 ms depending on the subject's stop success/failure (Rubia et al., 2005). There were 400 go trials and 87 stop trials.

In the PNC cohort, among the two available fMRI tasks, we chose to investigate the fractal  $n$ -back task due to its demands on cognitive control (Satterthwaite et al., 2014). In this task, subjects were presented with complex geometric figures (fractals) for 500 ms at a fixed 2500 ms inter-stimulus interval. In different block conditions, subjects pressed a button if they detected a predefined target fractal (0-back condition), if the current fractal was identical to the previous one (1-back condition), or if the current fractal was identical to the fractal 2 trials previously (2-back condition). Visual instructions (9 s) preceded each block informing the participant of the upcoming condition. Each condition was performed in three blocks of 20 trials (60 s) each. There were a total of 45 targets and 135 foils with 1:3 ratio in each block. A 24 s passive fixation period was presented at the beginning, middle, and end of the task.



**Tasks for behavioral assessments.** CPTs are available as part of larger cognitive test batteries in both cohorts. The Cambridge Neuropsychological Test Automated Battery (CANTAB; <http://www.cambridgecognition.com>) acquired in the IMAGEN cohort includes the rapid visual processing CPT task. This task requires subjects to detect a predefined target series of 3 digits in a continuous stream of digits (2–9) presented at a rate of 100/min. There were 27 occurrences of the target sequence during the 8 min experimental run. Accuracy in this task is commonly measured using performance accuracy ( $A'$ ) (Gau and Huang, 2014).  $A'$  is defined as  $0.5 + ((h - f) + (h - f)^2) / [4 \times h \times (1 - f)]$ , where  $h$  is the probability of hits and  $f$  is the probability of false alarms.  $A'$  is a signal detection measure of sensitivity to the target regardless of response tendency. It takes into account both hits and false alarms and is directly comparable to the classical index of sensitivity, performance accuracy ( $d'$ ) (see below; Sahgal, 1987). However, it is based on a nonparametric signal detection model suitable for the rapid visual processing task in which the sensory effects of stimulus triplets may not be well represented by the normal distribution. Difference in  $A'$  across genotypes was tested using multiple regression.

The Penn Computerized Neurocognitive Battery (Penn CNB) acquired in the PNC cohort includes the Penn Continuous Performance Test (Kurtz et al., 2001). This task presents a stream of seven-segment displays (connected horizontal and vertical lines) at a rate of 60/min. The subjects were required to press a button whenever the display formed a digit (first half of experiment) or a letter (second half of experiment). There were 60 occurrences of targets (30 digits and 30 letters) during a total of 6 min. Accuracy was measured as sensitivity to the target regardless of response tendency using the classical sensitivity index  $d' = Z(h) - Z(f)$ , where  $Z(p)$  is the inverse of the cumulative distribution function of the Gaussian distribution. Hit rates ( $h$ ) of 1 were replaced with  $(n - 0.5)/n$  and false alarm rates ( $f$ ) of 0 were replaced with  $0.5/n$ , where  $n$  is the number of targets or nontargets, respectively (Macmillan and Kaplan, 1985). Difference in  $d'$  across genotypes was tested using multiple regression.

### Statistical analysis

**fMRI preprocessing.** The fMRI data provided on the IMAGEN database were already slice timing corrected, motion corrected, and spatially normalized to MNI space using SPM8 (<http://www.fil.ion.ucl.ac.uk/spm/>). For PNC fMRI data, we applied motion correction and spatial normalization to MNI space using ANTs (<http://stnava.github.io/ANTs/>). Further preprocessing was equivalent across IMAGEN and PNC datasets, which included regressing out six linear head motion parameters, white matter, and CSF confounds (based on segmentation, thresholded at 95% tissue type probability), five principal components of high variance voxels derived using CompCor (Behzadi et al., 2007), and one-time sample-shifted variants, as well as discrete cosine functions (for high-pass filtering at 1/128 Hz) of all confound regressors. Our volumes of interest were large-scale networks defined using independent component analysis of resting-state functional connectivity in an independent dataset as available in the 90-region FIND lab atlas (Shirer et al., 2012). Large-scale functional networks defined on the basis of their intrinsic connectivity architecture during resting state provide volume delineation unbiased by particular task-related activation. To this end, the use of an independent atlas permits application of the same volume of interest to both cohorts. Note that no resting-state data were available for a subject-specific definition of networks for the majority of IMAGEN subjects. Time courses were extracted from all voxels across the brain areas of each network, averaged to yield one time course per network and normalized to z-scores.

In addition to accounting for head motion with the above-described motion parameters, their time-shifted variants and discrete cosine functions, we verified that head motion did not substantially contribute to between-group effects using mean framewise displacement (MFD) as a measure (Power et al., 2012). Relatively few volumes per subject showed displacement  $>3$  SDs above the average MFD across all subjects (IMAGEN 16.1 [3.6%]  $\pm$  30.7 volumes and PNC 10.9 [4.7%]  $\pm$  15.5 volumes per subject). Further, only few subjects had an MFD  $>3$  SDs over the group average MFD (25 [1.8%] of IMAGEN subjects and 5 [2.2%] PNC subjects). Therefore, we did not exclude any subjects or

fMRI volumes based on head motion. Direct contrast of MFD across genotypes ensured that head motion did not differ significantly among T/T, T/C, and C/C carriers ( $p > 0.4$  for all pairwise  $t$  tests in IMAGEN and PNC).

**fMRI general linear models.** Analyses were performed using in-house MATLAB code. In IMAGEN's stop signal task, successful go trials densely covered the experimental run and thus served as implicit baseline. The time course of all other events; that is, successfully inhibited stop trials, inhibition failures on stop trials, left–right errors on go trials, and errors of omission (not responded in time on go trials) were convolved with the canonical hemodynamic response function to yield regressors of interest. A general linear model was constructed with these regressors for each subject and each network's time course averaged across all the respective voxels (CO, frontoparietal, dorsal attention, and default mode networks) as response. An equivalent GLM analysis was performed for the whole brain using voxelwise time courses as response. The contrast of interest comprised the sum of the respective regression coefficient estimates. Errors of omission were absent in 20% of participants and very sparse in the other subjects and therefore were excluded from the contrast. At the group level, the resulting contrast value entered multiple regression with genotypes as regressor of interest.

The whole-brain voxelwise statistics in the IMAGEN cohort was derived by restricting the overdominance contrast volume (T/C carriers  $>$  other subjects) to the union of all 116 AAL atlas regions as lenient generic gray matter mask and applying an auxiliary uncorrected threshold of  $p < 0.005$  (two-sided  $t$  test) followed by cluster-level correction for multiple comparisons. Covariates of no interest were coregressed. The cluster size for this correction was determined using a Monte Carlo simulation with 1000 permutations of randomized genotypes using in-house MATLAB code.

In PNC's  $n$ -back task, regressors were generated by convolving the canonical hemodynamic response function with the boxcar time course of 0-back, 1-back, and 2-back blocks. In addition, we modeled preblock instructions (9 s) as an additional regressor of no interest to account for the respective brain processes. A general linear model was constructed with these regressors for each subject and the time course averaged across all the voxels of the network volume of interest as response. The contrast of interest comprised the sum of the regression coefficient estimates of 0-back, 1-back, and 2-back blocks. At the group level, the resulting contrast value was entered into multiple regression as response, with genotypes as regressor of interest.

For data quality assurance, subjects for which the estimated BOLD response in any of the network volumes-of-interest deviated by  $>3$  SDs from the mean were excluded from fMRI group statistics (33 subjects in IMAGEN, none in PNC).

**Group-level regression (fMRI and behavioral).** An initial model compared fMRI signal across rs1044396 genotypes with no a priori assumption on the genetic model of association using two binary regressors to encode genotypes, with the values 0 for T/T, 1 for T/C, and 0 for C/C. In subsequent models that specifically tested for presence of overdominance, a binary regressor with 1 encoding T/C carriers and 0 encoding T/T and C/C carriers was used, thus testing T/C heterozygotes against T/T and C/C homozygotes. For the IMAGEN cohort, covariates of no interest comprised sex, puberty score, scan site (seven categorical covariates) and population structure (first three principal components). For the PNC cohort, covariates of no interest included sex, age, and population structure (first three principal components).

## Results

CO network activation was investigated using fMRI of tasks that have high cognitive demands known to engage this network (Whelan et al., 2012; Satterthwaite et al., 2013). Behavior was studied using CPTs, the continuous nature of which is specifically designed and widely used to measure tonic alertness or vigilance selectively (Beck et al., 1956; Kurtz et al., 2001).

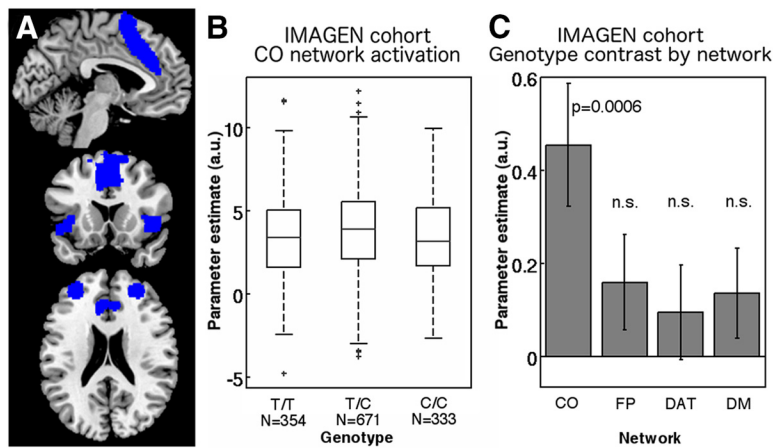


**Figure 1.** Heterozygotes at the *CHRNA4* SNP have increased CO network activation. **A**, CO network volume of interest in the FINDlab atlas based on intrinsic functional connectivity (Shirer et al., 2012). **B**, Estimated brain activation averaged across the CO network volume of interest in the IMAGEN cohort during the stop signal task. Higher CO network activation is observed in heterozygotes compared with homozygous T/T and C/C carriers. In boxes, the central mark indicates the median and the bottom and top edges indicate 25th and 75th percentiles, respectively. The whiskers extend to the most extreme data points not considered outliers (within 1.5 interquartile range of the bottom and top of box), and the outliers are marked by “+”. **C**, Genotype contrast T/C > homozygotes for activation in the CO network and three other networks for comparison: FP, Frontoparietal; DAT, dorsal attention; DM, default mode. A significant overdominant effect was observed for the CO network only. Error bars indicate SE.

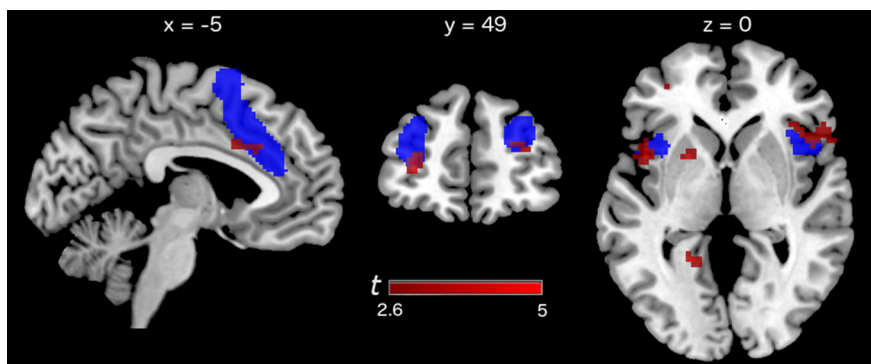


**Figure 2.** Whole-brain map showing that activation differences across genotypes overlap with the CO network. Shown is the contrast T/C larger than homozygous T/T and C/C carriers in the IMAGEN cohort during the stop signal task ( $p < 0.005$  auxiliary uncorrected threshold, corrected at cluster level). Blue shows the CO volume of interest as in Figure 1; red shows areas of higher activation in heterozygotes displayed on a canonical single subject structural image demonstrating the overlap in dorsal anterior cingulate, anterior prefrontal, and anterior insula loci.

### *CHRNA4* polymorphism and CO network activation

We hypothesized that activity in the CO network during cognitive engagement is affected by rs1044396 genotype. The CO network volume of interest was taken from a functional atlas derived from resting-state functional connectivity analysis of an independent sample (Fig. 1A) (Shirer et al., 2012). In the IMAGEN fMRI dataset ( $n = 1358$ ; Table 1), we investigated network activity during a stop signal task that requires a high level of cognitive control. Subjects had to press a button in response to regularly presented go stimuli but withhold response if the go stimulus was followed by a stop signal. Note that, although this task requires several other cognitive control functions such as top-down inhibition and spatial attention, it is known to heavily involve tonic alertness and the CO network (Satterthwaite et al., 2013). For each subject, the CO network fMRI signal time course was entered in a general linear model comprising regressors for all estimable task events. Estimated brain activity across these events confirmed strong engagement of the CO network volume of interest across all subjects regardless of genotype (one-sample

$t$  test  $t_{(1357)} = 54.57$ ,  $p < 10^{-10}$ ). With T/T (homozygous carriers of the major allele) as the baseline, we examined the effects of the presence of minor allele C; that is, T/C and C/C genotypes, on CO network activity using multiple regression with no a priori assumption on the genetic model of association. Task-related activity in this network was significantly higher in T/C carriers compared with T/T carriers ( $t_{(1343)} = 2.83$ ,  $p = 0.005$ ; Fig. 1), whereas activity for C/C carriers did not differ from T/T carriers ( $t_{(1343)} = -0.003$ ,  $p = 0.998$ ). This result is suggestive of an overdominant effect in which the phenotype of heterozygotes lies outside the phenotypic range of both homozygous groups due to allelic interaction at a single locus (Hochholdinger and Hoecker, 2007). After this observation, we used multiple regression to test specifically for overdominance; that is, T/C carriers > all other subjects. This analysis confirmed higher CO network activity in heterozygotes compared with homozygotes ( $t_{(1344)} = 3.44$ ,  $p = 0.0006$ , 0.9% variance explained).

To test the neuroanatomical specificity of the rs1044396 impact on the CO network, we investigated three other high-level networks as controls. These comprised the default mode network as well as two networks underlying other cognitive control functions, namely the dorsal attention network supporting selective attention and the lateral frontoparietal network supporting phasic adaptive control. Using identical first- and second-level GLM analyses, neither T/C nor C/C carriers showed significant differences in network activation compared with T/T carriers in these three control networks (all  $t_{(1343)} < 1.2$ ), nor was an effect observed when comparing T/C against both homozygous groups (all  $t_{(1344)} < 1.6$ ; Fig. 1C).

To further investigate this neuroanatomical specificity, we complemented our volume of interest-based approach with whole-brain voxelwise regression. Contrasting T/C carriers with homozygotes, we found significantly higher activity in T/C carriers across several cortical areas of the CO network (cluster-level corrected based on Monte Carlo permutation test after an auxiliary uncorrected threshold  $p < 0.005$ ). These nodes comprised right and left anterior insulae, right and left anterior prefrontal cortices, and left dorsal anterior cingulate cortex (Fig. 2, Table 2). The clusters showed anatomical overlap and correspondence with all five cortical areas of the CO network as defined by the FIND atlas (Shirer et al., 2012). We found additional significant clusters largely located in sensory and motor processing regions (Table 2) that may represent task-specific processing top-down modulated by higher cognitive control engagement of the CO network in heterozygotes.

We tested whether an overdominant effect could be confirmed in the independent PNC fMRI dataset ( $n = 228$ ). This cohort completed an  $n$ -back task that requires subjects to moni-

**Table 2. Contrasting task-evoked activity between T/C carriers and homozygotes**

	MNI <i>x, y, z</i> coordinates	Peak $t_{(1344)}$	Peak <i>p</i>	Cluster size (voxels)	Corrected cluster <i>p</i> *
<b>CO network</b>					
Anterior insula					
Right	36 20 -5	4.22	$<5 * 10^{-5}$	95	0.0004
Left	-45 11 -2	4.16	$<5 * 10^{-5}$	54	0.002
Left	-33 17 -8	4.52	$<5 * 10^{-5}$	14	0.040
Anterior prefrontal					
Right	30 47 19	3.52	$<5 * 10^{-4}$	14	0.040
Left	-30 50 7	4.50	$<5 * 10^{-5}$	22	0.017
Dorsal anterior cingulate, left	-6 23 31	3.50	$<5 * 10^{-4}$	13	0.046
<b>Non-CO regions</b>					
Precentral gyrus					
Left	-51 -10 40	4.0	$<5 * 10^{-5}$	38	0.005
Right	33 -25 49	4.43	$<5 * 10^{-5}$	19	0.023
Right, inferior	57 -1 24	3.81	$<5 * 10^{-4}$	17	0.028
Cuneus, right	18 -78 31	3.68	$<5 * 10^{-4}$	30	0.010
Lingual gyrus, left	-18 -49 4	4.16	$<5 * 10^{-5}$	28	0.010
Putamen, left	-21 8 4	3.83	$<5 * 10^{-4}$	20	0.021
Superior temporal gyrus, left	-66 -37 17	3.83	$<5 * 10^{-4}$	18	0.025

\*Permutation-based after an auxiliary uncorrected threshold  $p < 0.005$ .

tor a continuous stream of abstract geometric images for specific stimulus repeats. In different block conditions, subjects pressed a button if they detected a predefined target image (0-back condition), if the current image was identical to the previous one (1-back condition), or if the current image was identical to the image 2 trials previously (2-back condition). Again, we investigated brain activity evoked by all estimable events (0-back, 1-back, and 2-back trials). Strong engagement of the CO network was confirmed across all subjects regardless of genotype (one-sample  $t$  test  $t_{(227)} = 12.50$ ,  $p < 10^{-10}$ ). Activation in the CO network was then compared across subjects with rs1044396 T/T, T/C, and C/C genotypes (Fig. 3A). Using multiple regression, we tested for overdominance; that is, T/C carriers  $>$  all other subjects. This analysis confirmed higher CO network activation in heterozygotes compared with homozygotes ( $t_{(221)} = 2.77$ ,  $p = 0.006$ , 3.4% variance explained).

Note that, beyond increased demands on tonic alertness, the  $n$ -back task requires considerable working memory engagement. This task is thus commonly used to extract working memory processes associated with regions of the frontoparietal network, especially the dorsolateral prefrontal cortex (Owen et al., 2005; D'Esposito and Postle, 2015). Indeed, whereas the frontoparietal network was activated by this task (one-sample  $t$  test regardless of genotype  $t_{(227)} = 4.31$ ,  $p < 10^{-4}$ ), no significant activation difference was found across genotypes in this network or the other two networks, dorsal attention and default mode networks, that we investigated as controls (all  $t_{(221)} < 0.8$  for T/C against homozygotes; Fig. 3B). This result again speaks to the anatomical specificity of the impact of rs1044396 on CO network activation.

### CHRNA4 rs1044396 and tonic alertness

After observing that the rs1044396 polymorphism is associated with the strength of activation in brain areas maintaining tonic alertness, we next investigated whether this impact translates into interindividual differences in behavioral measures of tonic alertness. Tonic alertness, the intrinsically maintained preparedness to process information and to respond, is a necessary prerequisite for more specialized cognitive functions such as selective attention and perceptual processes to build on. In contrast to selective

attention and phasic stimulus-driven alertness, tonic alertness is continuous rather than transient (Posner and Boies, 1971) and has a general overarching nature, rather than operating with respect to specific information and sensory features (Robertson and Garavan, 2004).

Note that the tasks for which fMRI data were available coengaged multiple higher-order cognitive processes, rendering the selective investigation of alertness difficult. Therefore, to study behavior, we turned instead to behavioral CPTs that target tonic alertness selectively. The IMAGEN study contains a visual CPT called rapid visual processing, during which subjects ( $n = 1499$ ) continuously attend a visual stream of digits and press a button whenever a predefined target sequence of three digits is detected.  $A'$  was compared across rs1044396 genotypes (Fig. 4A). Paralleling the neuroimaging findings, we tested for presence of overdominance (i.e., T/C carriers  $>$  all other subjects) and found that heterozygotes showed the highest performance accuracy ( $t_{(1485)} = 2.28$ ,  $p = 0.023$ , 0.4% variance explained). For completeness, we also investigated behavior comprehensively during the fMRI SST task (individual stop signal delay, stop signal reaction time, reaction time on go trials, failures to stop, and left–right errors). We found no significant impact of genotype, presumably because of dependence of performance in this task on multiple overlapping cognitive control faculties, consistent with a lack of behavioral effects during the two previous neuroimaging studies of rs1044396 (Winterer et al., 2007; Giessing et al., 2012).

We then attempted to replicate the presence of overdominance at rs1044396 on behavior in the independent PNC cohort. PNC uses a visual CPT during which subjects ( $n = 2151$ ) continuously attend a visual stream of figures made of seven lines and press a button whenever the lines form a digit or a letter.  $d'$  was compared across subjects with rs1044396 T/T, T/C, and C/C genotypes (Fig. 4B). This analysis confirmed higher performance accuracy in heterozygotes compared with T/T and C/C carriers ( $t_{(2144)} = 3.18$ ,  $p = 0.0015$ , 0.5% variance explained).

### Meta-analysis of overdominance

Finally, to investigate the cumulative evidence gained from IMAGEN and PNC cohorts for overdominance at rs1044396 (T/C  $>$  [T/T C/C]) in fMRI and behavioral data, we performed a meta-analysis over the respective effect sizes. We found that  $z = 4.36$ ,  $p = 1.33 * 10^{-5}$  (total  $n = 1586$ ) for the fMRI measures of CO activation and  $z = 2.54$ ,  $p = 0.011$  (total  $n = 3650$ ) for behavioral measures of alertness. The behavioral meta-analysis underperformed compared with the fMRI meta-analysis, presumably due to the heterogeneity of the behavioral measure across the two cohorts (behavioral:  $q = 8.88$ ,  $p = 0.003$ ; fMRI:  $q = 0.5$ ,  $p = 0.48$ ).

### CHRNA4 overdominance and haplotypes

To further elucidate whether the observed overdominant effect was due to allelic interaction at the SNP of interest or if it was the result of heterozygosity at multiple neighboring locations (pseudoverdominance, see Discussion section), we performed haplotype association tests for the LD block surrounding rs1044396, which includes 28 SNPs. Eleven haplotypes with frequency  $> 1\%$  were considered for the analysis. Haplotype frequencies are comparable between IMAGEN and PNC, with the H1 haplotype, which includes the rs1044396-T allele, being the most frequent (38%) in both the IMAGEN and PNC cohorts. We found no significant association of CO network activation levels or behavioral measures of alertness for haplotypes of the surrounding *CHRNA4* region in either cohort (the omnibus tests were not significant



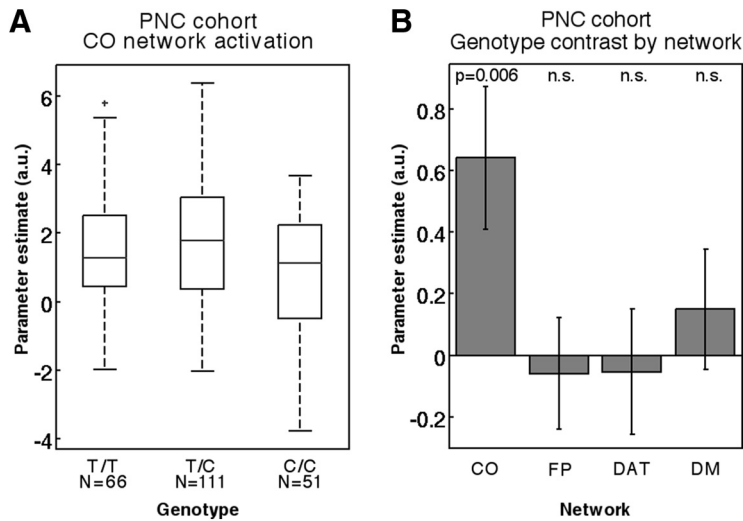


**Figure 3.** Increased CO network activation in heterozygotes is replicated in the PNC cohort. **A**, Estimated brain activation averaged across the CO network volume of interest in the PNC cohort during the fractal  $n$ -back task is shown separately for each genotype. Higher CO network activation is observed in heterozygotes compared with homozygous T/T and C/C carriers. Box plots are arranged as explained in Figure 1. **B**, Genotype contrast T/C > homozygotes is shown for activation in the CO network and three other networks for comparison (abbreviations as in Fig. 1). A significant overdominant effect was observed for the CO network only. Error bars indicate SE.

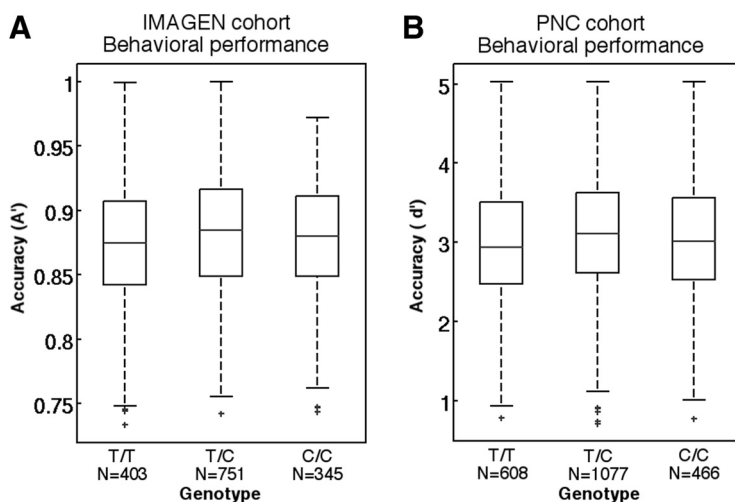


**Figure 4.** Impact of genotype on tonic alertness capacity shows an overdominant effect. Performance accuracy in CPTs as measured by perceptual sensitivity is shown for the IMAGEN (**A**) and PNC (**B**) cohorts for the three rs1044396 genotypes. In both datasets, heterozygotes performed better than homozygote carriers of the major ("T") or minor ("C") allele. Box plots are arranged as explained in Figure 1.

and no individual haplotype showed a significant association). This result speaks against pseudo-overdominance in favor of a true overdominant effect at rs1044396.

#### *CHRNA4* rs1044396 and gene expression levels

The potential biological mechanisms underlying the observed impact of the synonymous SNP rs1044396 remains unclear. Although the SNP has no effect on the amino acid level, the change from T to C disrupts a potential methylation site (CpG). Indeed, the entire exon 5 of *CHRNA4* overlaps with a CpG island (UCSC genome browser; Kent et al., 2002). Therefore, we investigated the dependence of *CHRNA4* expression in neural tissue on this polymorphism using publicly available data from the Genotype-Tissue Expression (GTEx) project (GTEx Consortium, 2015). Based on the focus of our neuroimaging investigations on large-

scale cortical networks, we investigated the two available cortical regions Brodmann area (BA) 9 (samples = 92; in the vicinity to BA46 that encompasses the anterior prefrontal region of CO network; cf. Fig. 1A) and BA 24 (samples = 72; directly overlapping with the anterior cingulate cortex region of the CO network). In addition, we analyzed the tibial nerve because much higher tissue samples were available for it compared with brain tissues (samples = 256). In all investigated neural tissue, we found a linear dosage effect such that homozygous major allele carriers (T/T) had the highest expression levels and heterozygotes showed intermediate gene expression (BA 9  $t = 4.3$ ,  $p = 6 \times 10^{-5}$ , BA 24  $t = 2.6$ ,  $p = 0.011$ ; tibial nerve  $t = 5.4$ ,  $p = 2 \times 10^{-7}$ ). This analysis shows that rs1044396 is an expression quantitative trait locus (eQTL) modulating the expression levels of *CHRNA4*.

#### Discussion

Although the nicotinic system plays an important role in cognitive control processes, the contribution of genetic variability in this system to (nicotine consumption-unrelated) cognition has received scant attention (Greenwood et al., 2012). Furthermore, it is not well understood whether any specific brain structures are affected by the genetic makeup of the nicotinic system. Here, we investigated the relation between brain activity and behavior with a common SNP of the most prevalent, high-affinity nicotinic receptor in the brain. Specifically, based on our prior findings of nicotinic receptor distribution (Picard et al., 2013), we expected the rs1044396 genotype to affect neural activity in the CO network. In addition, based on the previously established link between the CO network and sustained alertness (Sadaghiani and D'Esposito, 2015), we expected an impact of this polymorphism on the ability to engage this cognitive control function. The CO network is known to show pervasive activation across numerous distinct cognitive tasks. This general activation profile allowed us to study the CO network in previously acquired fMRI experiments across two large cohorts. We found that, during cognitive engagement, the CO network, but not other control-related networks, showed higher activity in heterozygotes (T/C carriers) compared with homozygous carriers of the major (T/T) or minor allele (C/C). Furthermore, we observed that heterozygotes performed at significantly higher accuracy in behavioral tasks that primarily depend on the ability to maintain alertness. Findings were consistent across both cohorts totaling  $N = 1586$  subjects for neuroimaging and  $N = 3650$  for behavior. These results therefore expand considerably upon encouraging, but relatively underpowered ( $N < 50$ ), neuroimaging studies of this SNP (Winterer et al., 2007; Giessing et al., 2013). One of these

studies found the highest task-related activity in T/T homozygotes in supplementary motor/anterior cingulate cortex and left postcentral gyrus (Winterer et al., 2007). Conversely, the other study, which did not include heterozygous subjects, found higher activity for C/C compared with T/T carriers in right middle temporal, but lower activity in right superior temporal gyrus (Giessing et al., 2012). Our results constitute the first report of overdominance in a *CHRNA4* association study of brain activity and cognitive performance. This overdominant effect may be one contributor to discrepancy in impact from T versus C alleles in previous behavioral and fMRI studies with smaller sample sizes.

### Possible mechanisms underlying overdominance

What could be driving the observed overdominant effect? Overdominance is often missed because the most prevalent genetic models used in genome-wide association studies rely on the a priori assumption that alleles contribute to complex traits in a linear additive fashion. However, overdominance is expected to be very prevalent (Comings and MacMurray, 2000). One common source of overdominance is thought to be the interaction among multimeric protein products (Comings and MacMurray, 2000). The  $\alpha 4\beta 2$  nicotinic receptor is a pentamer and commonly contains two  $\alpha 4$  subunits, readily suggesting functional interactions between these subunits. However, rs1044396 leads to a synonymous amino acid substitution and it seems unlikely that such modification would affect  $\alpha 4$  multimerization. A more plausible explanation could relate to a pseudo-overdominant effect (Draghi and Whitlock, 2015) due to the presence of multiple *cis*-acting *CHRNA4* SNPs in the LD block, including rs1044396, which may favor the expression of a particular haplotype overrepresented in rs1044396 heterozygotes. However, according to our haplotype analysis, we can exclude the existence of *cis*-interacting SNPs at the rs1044396-LD block. At the same time, we should not ignore the possibility of a hidden interaction between rs1044396 and another genetic/environmental factor (e.g., a SNP  $\times$  SNP interaction or an SNP  $\times$  environment interaction). The possibility of an SNP  $\times$  environment interaction is supported by the fact that rs1044396 is followed by a “G” nucleotide, thus creating a potential methylation site (CpG) in rs1044396 C-allele carriers that is absent in rs1044396 T-allele carriers.

### Overdominance and functional advantage of intermediate expression levels

A source for overdominance at rs1044396 could be an advantage of intermediate *CHRNA4* expression levels, possibly modulated by the methylation site. One of the best-known examples of overdominance is the nonsynonymous (Val $\rightarrow$ Met) SNP rs4680 of the *COMT* gene. *COMT* encodes the dopamine-metabolizing enzyme catechol-O-methyltransferase, with the Met variant (T-allele) showing a dosage effect on prefrontal dopamine concentrations. Association of cognitive performance with prefrontal dopamine often follows an inverted U shape. Therefore, intermediate dopamine levels observed in heterozygous carriers result in better performance in specific cognitive tasks compared with homozygous C/C and T/T carriers (Cools and D’Esposito, 2011). An analogous effect could underlie our overdominance observations of *CHRNA4*, such that having one rs1044396 T-allele would result in intermediate expression levels of the corresponding  $\alpha 4$  protein. This interpretation is strongly supported by our finding that rs1044396 is an eQTL for *CHRNA4*, resulting in intermediate gene expression levels in heterozygotes. Because *CHRNA4* likely affects receptor sensitivity to acetylcholine (Eggert et al., 2015), intermediate expression levels might be optimal for certain func-

tions such as those underlying maintenance of tonic alertness, resulting in heterosis (superior phenotype of heterozygotes).

The optimal expression level, however, might be dependent on the cognitive function under investigation. In the context of *COMT*, the ideal prefrontal dopamine level (i.e., the peak of the inverted U-shape function) is task dependent, resulting in discrepancies across *COMT* association studies (Cools and D’Esposito, 2011). An inverted U function could drive a similar task dependence for rs1044396 effects and explain the contradictory reports in behavioral association studies (Störmer et al., 2012). Although the high density of  $\alpha 4\beta 2$  receptors in the CO network suggests an especially prominent role of *CHRNA4* polymorphisms in sustained alertness, other cognitive control functions are likely affected as well. The association of rs1044396 genotype with performance might differ for tasks that primarily rely on sustained alertness (such as the CPT tasks studied here) compared with those targeting phasic and selective control functions such as spatial attention or cued orienting investigated in previous studies (Greenwood et al., 2005, 2005; Espeseth et al., 2010). Such task dependence may also explain the different findings in the two previous brain imaging studies of rs1044396 that focused on selective attention tasks (Winterer et al., 2007; Giessing et al., 2012).

### Limitations

One limitation to making use of previously acquired datasets is that we were not able to administer an ideal task specific to tonic alertness during fMRI. Rather, we had to interrogate tonic alertness as a cognitive control function that was common to the cognitively demanding tasks examined here. The available neuroimaging tasks heavily involved more specific functions such as response inhibition (stop signal task in IMAGEN) and working memory (*n*-back task in PNC) in addition. This coengagement of cognitive functions limits an unequivocal interpretation of the neuroimaging effects as tonic alertness. However, the fact that two very different tasks resulted in comparable overdominant effects supports the interpretation that rs1044396 affects an omnipresent cognitive control function shared across the respective tasks. The observation of overdominant effects in behavioral CPT procedures that selectively target tonic alertness suggests that this general control function might constitute alertness.

Another potential limitation of our study, and a difference from previous association studies of rs1044396, is the subjects’ age. The IMAGEN and PNC cohorts consist of adolescents and young adults, whereas the average age in previous behavioral studies has commonly spanned the mid-30 s and higher (Greenwood et al., 2005; Parasuraman et al., 2005; Reinvang et al., 2009). It is conceivable that the genotype effects observed in our cohorts change across the lifespan beyond the age range that we investigated. This question should be addressed in future studies using neuroimaging and genetics cohorts at other ages. A potential difference in the *CHRNA4* genotype effect between teenaged subjects and older subjects would provide an important step forward in understanding genetic contributions to individual brain development during puberty.

Finally, the hypothesis-driven investigation of a single common SNP may present a potential limitation in terms of overall functional impact. Common SNPs generally have small effect sizes and are only a small piece of a large picture in the explanation of complex traits and their neural substrate.

### Conclusions

In this association study of the high-affinity nicotinic receptor  $\alpha 4\beta 2$  in two large cohorts, we establish the importance of the CO



network in mediating the neuromodulatory effects of acetylcholine on cognition. We further provide a piece of the genetic puzzle underlying interindividual differences in the foundational ability to maintain alertness. These insights into the role of genetic variability in brain activation and cognitive control may help us to understand how genetic changes translate into aberrant behavior in various disorders of cognitive control. This line of work may facilitate individualized medicine in the future by informing how particular neuropharmacological treatments will affect individual patients' brain activity and cognition based on their genotype. The specific study of nicotinic receptors can further lend insights into the basis of individuals' susceptibility to nicotine addiction as it depends on brain activity and cognitive control profile. In summary, the current findings establish a connection between *CHRNA4* genotype, CO network activation, and sustained alertness, providing insights into brain–behavior relations and how genetics shape them.

## References

- Albuquerque EX, Pereira EF, Alkondon M, Rogers SW (2009) Mammalian nicotinic acetylcholine receptors: from structure to function. *Physiol Rev* 89:73–120. [CrossRef Medline](#)
- Barrett JC, Fry B, Maller J, Daly MJ (2005) Haploview: analysis and visualization of LD and haplotype maps. *Bioinformatics* 21:263–265. [CrossRef Medline](#)
- Beck LH, Bransome ED Jr, Mirsky AF, Rosvold HE, Sarason I (1956) A continuous performance test of brain damage. *J Consult Psychol* 20:343–350. [CrossRef Medline](#)
- Behzadi Y, Restom K, Liu J, Liu TT (2007) A component based noise correction method (CompCor) for BOLD and perfusion based fMRI. *Neuroimage* 37:90–101. [CrossRef Medline](#)
- Breitling LP, Dahmen N, Mittelstrass K, Rujescu D, Gallinat J, Fehr C, Giegling I, Lamina C, Illig T, Müller H, Raum E, Rothenbacher D, Wichmann HE, Brenner H, Winterer G (2009) Association of nicotinic acetylcholine receptor subunit  $\alpha 4$  polymorphisms with nicotine dependence in 5500 Germans. *Pharmacogenomics* 9:219–224. [CrossRef Medline](#)
- Chang Z, Lichtenstein P, Asherson PJ, Larsson H (2013) Developmental twin study of attention problems: high heritabilities throughout development. *JAMA Psychiatry* 70:311–318. [CrossRef Medline](#)
- Comings DE, MacMurray JP (2000) Molecular heterosis: a review. *Mol Genet Metab* 71:19–31. [CrossRef Medline](#)
- Cools R, D'Esposito M (2011) Inverted-U-shaped dopamine actions on human working memory and cognitive control. *Biol Psychiatry* 69:e113–e125. [CrossRef Medline](#)
- Das S, et al. (2016) Next-generation genotype imputation service and methods. *Nat Genet* 48:1284–1287. [CrossRef Medline](#)
- Delaneau O, Zagury JF, Marchini J (2013) Improved whole-chromosome phasing for disease and population genetic studies. *Nat Methods* 10:5–6. [CrossRef Medline](#)
- D'Esposito M, Postle BR (2015) The cognitive neuroscience of working memory. *Annu Rev Psychol* 66:115–142. [CrossRef Medline](#)
- Dosenbach NU, Visscher KM, Palmer ED, Miezin FM, Wenger KK, Kang HC, Burgund ED, Grimes AL, Schlaggar BL, Petersen SE (2006) A core system for the implementation of task sets. *Neuron* 50:799–812. [CrossRef Medline](#)
- Draghi J, Whitlock MC (2015) Overdominance interacts with linkage to determine the rate of adaptation to a new optimum. *J Evol Biol* 28:95–104. [CrossRef Medline](#)
- Durbin R (2014) Efficient haplotype matching and storage using the positional Burrows–Wheeler transform (PBWT). *Bioinformatics* 30:1266–1272. [CrossRef Medline](#)
- Eggert M, Winterer G, Wanischek M, Hoda JC, Bertrand D, Steinlein O (2015) The nicotinic acetylcholine receptor alpha 4 subunit contains a functionally relevant SNP Haplotype. *BMC Genet* 16:46. [CrossRef Medline](#)
- Espeseth T, Sneve MH, Rootwelt H, Laeng B (2010) Nicotinic receptor gene *CHRNA4* interacts with processing load in attention. *PLoS One* 5:e14407. [CrossRef Medline](#)
- Feng Y, Niu T, Xing H, Xu X, Chen C, Peng S, Wang L, Laird N, Xu X (2004) A common haplotype of the nicotine acetylcholine receptor  $\alpha 4$  subunit gene is associated with vulnerability to nicotine addiction in men. *Am J Hum Genet* 75:112–121. [CrossRef Medline](#)
- Friedman NP, Miyake A, Young SE, Defries JC, Corley RP, Hewitt JK (2008) Individual differences in executive functions are almost entirely genetic in origin. *J Exp Psychol Gen* 137:201–225. [CrossRef Medline](#)
- Gallezot JD, Bottlaender M, Grégoire MC, Roumenov D, Deverre JR, Coulon C, Ottaviani M, Dollé F, Syrota A, Valette H (2005) In vivo imaging of human cerebral nicotinic acetylcholine receptors with 2-18F-fluoro-A-85380 and PET. *J Nucl Med* 46:240–247. [Medline](#)
- Gau SS, Huang WL (2014) Rapid visual information processing as a cognitive endophenotype of attention deficit hyperactivity disorder. *Psychol Med* 44:435–446. [CrossRef Medline](#)
- Giessing C, Neber T, Thiel CM (2012) Genetic variation in nicotinic receptors affects brain networks involved in reorienting attention. *Neuroimage* 59:831–839. [CrossRef Medline](#)
- Giessing C, Thiel CM, Alexander-Bloch AF, Patel AX, Bullmore ET (2013) Human brain functional network changes associated with enhanced and impaired attentional task performance. *J Neurosci* 33:5903–5914. [CrossRef Medline](#)
- Greenwood PM, Fossella JA, Parasuraman R (2005) Specificity of the effect of a nicotinic receptor polymorphism on individual differences in visuospatial attention. *J Cogn Neurosci* 17:1611–1620. [CrossRef Medline](#)
- Greenwood PM, Parasuraman R, Espeseth T (2012) A cognitive phenotype for a polymorphism in the nicotinic receptor gene *CHRNA4*. *Neurosci Biobehav Rev* 36:1331–1341. [CrossRef Medline](#)
- Gruszka A, Matthews G, Szymura B (2010) Handbook of individual differences in cognition: attention, memory, and executive control. New York: Springer Science and Business Media.
- Hendrickson LM, Guildford MJ, Tapper AR (2013) Neuronal nicotinic acetylcholine receptors: common molecular substrates of nicotine and alcohol dependence. *Front Psychiatry* 4:29. [CrossRef Medline](#)
- Higley MJ, Picciotto MR (2014) Neuromodulation by acetylcholine: examples from schizophrenia and depression. *Curr Opin Neurobiol* 29:88–95. [CrossRef Medline](#)
- Hochholdinger F, Hoecker N (2007) Towards the molecular basis of heterosis. *Trends Plant Sci* 12:427–432. [CrossRef Medline](#)
- Kent WJ, Sugnet CW, Furey TS, Roskin KM, Pringle TH, Zahler AM, Haussler D (2002) The Human Genome Browser at UCSC. *Genome Res* 12:996–1006. [CrossRef Medline](#)
- Knott V, Bosman M, Mahoney C, Iivitsky V, Quirt K (1999) Transdermal nicotine: single dose effects on mood, EEG, performance, and event-related potentials. *Pharmacol Biochem Behav* 63:253–261. [CrossRef Medline](#)
- Kozak R, Bruno JP, Sarter M (2006) Augmented prefrontal acetylcholine release during challenged attentional performance. *Cereb Cortex* 16:9–17. [Medline](#)
- Kurtz MM, Ragland JD, Bilker W, Gur RC, Gur RE (2001) Comparison of the continuous performance test with and without working memory demands in healthy controls and patients with schizophrenia. *Schizophr Res* 48:307–316. [CrossRef Medline](#)
- Lesh TA, Niendam TA, Minzenberg MJ, Carter CS (2011) Cognitive control deficits in schizophrenia: mechanisms and meaning. *Neuropsychopharmacology* 36:316–338. [CrossRef Medline](#)
- Loh PR, Danecek P, Palamara PF, Fuchsberger C, A Reshef Y, K Finucane H, Schoenherr S, Forer L, McCarthy S, Abecasis GR, Durbin R, L Price A (2016) Reference-based phasing using the Haplotype Reference Consortium panel. *Nat Genet* 48:1443–1448. [CrossRef Medline](#)
- Macmillan NA, Kaplan HL (1985) Detection theory analysis of group data: estimating sensitivity from average hit and false-alarm rates. *Psychol Bull* 98:185–199. [CrossRef Medline](#)
- Mägi R, Morris AP (2010) GWAMA: software for genome-wide association meta-analysis. *BMC Bioinformatics* 11:288. [CrossRef Medline](#)
- McCarthy S (2016) A reference panel of 64,976 haplotypes for genotype imputation. *Nat Genet* 48:1279–1283. [CrossRef Medline](#)
- Mennes M, Zuo XN, Kelly C, Di Martino A, Zang YF, Biswal B, Castellanos FX, Milham MP (2011) Linking inter-individual differences in neural activation and behavior to intrinsic brain dynamics. *Neuroimage* 54:2950–2959. [CrossRef Medline](#)
- Owen AM, McMillan KM, Laird AR, Bullmore E (2005) N-back working memory paradigm: A meta-analysis of normative functional neuroimaging studies. *Hum Brain Mapp* 25:46–59. [CrossRef Medline](#)
- Parasuraman R (1998) *The attentive brain*. Cambridge, MA: MIT.

- Parasuraman R, Greenwood PM, Kumar R, Fossella J (2005) Beyond heritability neurotransmitter genes differentially modulate visuospatial attention and working memory. *Psychol Sci* 16:200–207. [CrossRef Medline](#)
- Petersen AC, Crockett L, Richards M, Boxer A (1988) A self-report measure of pubertal status: reliability, validity, and initial norms. *J Youth Adolesc* 17:117–133. [CrossRef Medline](#)
- Picard F, Sadaghiani S, Leroy C, Courvoisier DS, Maroy R, Bottlaender M (2013) High density of nicotinic receptors in the cingulo-insular network. *Neuroimage* 79:42–51. [CrossRef Medline](#)
- Posner MI (2008) Measuring alertness. *Ann N Y Acad Sci* 1129:193–199. [CrossRef Medline](#)
- Posner MI, Boies SJ (1971) Components of attention. *Psychol Rev* 78:391–408. [CrossRef](#)
- Power JD, Barnes KA, Snyder AZ, Schlaggar BL, Petersen SE (2012) Spurious but systematic correlations in functional connectivity MRI networks arise from subject motion. *Neuroimage* 59:2142–2154. [CrossRef Medline](#)
- Reinvang I, Lundervold AJ, Rootwelt H, Wehling E, Espeseth T (2009) Individual variation in a cholinergic receptor gene modulates attention. *Neurosci Lett* 453:131–134. [CrossRef Medline](#)
- Robertson IH, Garavan H (2004) Vigilant attention. In: *The cognitive neurosciences*, Ed 3, pp 563–578. Cambridge, MA: MIT.
- Rubia K, Smith AB, Brammer MJ, Toone B, Taylor E (2005) Abnormal brain activation during inhibition and error detection in medication-naïve adolescents with ADHD. *Am J Psychiatry* 162:1067–1075. [CrossRef Medline](#)
- Sadaghiani S, D'Esposito M (2015) Functional characterization of the cingulo-opercular network in the maintenance of tonic alertness. *Cereb Cortex* 25:2763–2773. [CrossRef Medline](#)
- Sadaghiani S, Scheeringa R, Lehongre K, Morillon B, Giraud AL, Kleinschmidt A (2010) Intrinsic connectivity networks, alpha oscillations, and tonic alertness: a simultaneous electroencephalography/functional magnetic resonance imaging study. *J Neurosci* 30:10243–10250. [CrossRef Medline](#)
- Sahgal A (1987) Some limitations of indices derived from signal detection theory: evaluation of an alternative index for measuring bias in memory tasks. *Psychopharmacology (Berl)* 91:517–520. [CrossRef Medline](#)
- Sarter M, Paolone G (2011) Deficits in attentional control: cholinergic mechanisms and circuitry-based treatment approaches. *Behav Neurosci* 125:825–835. [CrossRef Medline](#)
- Satterthwaite TD, Elliott MA, Gerraty RT, Ruparel K, Loughhead J, Calkins ME, Eickhoff SB, Hakonarson H, Gur RC, Gur RE, Wolf DH (2013) An improved framework for confound regression and filtering for control of motion artifact in the preprocessing of resting-state functional connectivity data. *Neuroimage* 64:240–256. [CrossRef Medline](#)
- Satterthwaite TD, Elliott MA, Ruparel K, Loughhead J, Prabhakaran K, Calkins ME, Hopson R, Jackson C, Keefe J, Riley M, Mentch FD, Sleiman P, Verma R, Davatzikos C, Hakonarson H, Gur RC, Gur RE (2014) Neuroimaging of the Philadelphia Neurodevelopmental Cohort. *Neuroimage* 86:544–553. [CrossRef Medline](#)
- Satterthwaite TD, Connolly JJ, Ruparel K, Calkins ME, Jackson C, Elliott MA, Roalf DR, Ryan Hopsona KP, Behr M, Qiu H, Mentch FD, Chiavacci R, Sleiman PM, Gur RC, Hakonarson H, Gur RE (2016) The Philadelphia Neurodevelopmental Cohort: a publicly available resource for the study of normal and abnormal brain development in youth. *Neuroimage* 124:1115–1119. [CrossRef Medline](#)
- Schumann G, et al. (2010) The IMAGEN study: reinforcement-related behaviour in normal brain function and psychopathology. *Mol Psychiatry* 15:1128–1139. [CrossRef Medline](#)
- Seeley WW, Menon V, Schatzberg AF, Keller J, Glover GH, Kenna H, Reiss AL, Greicius MD (2007) Dissociable intrinsic connectivity networks for salience processing and executive control. *J Neurosci* 27:2349–2356. [CrossRef Medline](#)
- Shirer WR, Ryali S, Rykhlevskaia E, Menon V, Greicius MD (2012) Decoding subject-driven cognitive states with whole-brain connectivity patterns. *Cereb Cortex* 22:158–165. [CrossRef Medline](#)
- Störmer VS, Passow S, Biesenack J, Li SC (2012) Dopaminergic and cholinergic modulations of visual-spatial attention and working memory: insights from molecular genetic research and implications for adult cognitive development. *Dev Psychol* 48:875–889. [CrossRef Medline](#)
- Sturm W, Longoni F, Fimm B, Dietrich T, Weis S, Kemna S, Herzog H, Willmes K (2004) Network for auditory intrinsic alertness: a PET study. *Neuropsychologia* 42:563–568. [CrossRef Medline](#)
- Tanner JM (1978) *Growth at adolescence*, Ed 2. Springfield, IL: Blackwell Science.
- 1000 Genomes Project Consortium (2015) A global reference for human genetic variation. *Nature* 526:68–74. [CrossRef Medline](#)
- GTEx Consortium (2015) The Genotype-Tissue Expression (GTEx) pilot analysis: multitissue gene regulation in humans. *Science* 348:648–660. [CrossRef Medline](#)
- Whelan R, et al. (2012) Adolescent impulsivity phenotypes characterized by distinct brain networks. *Nat Neurosci* 15:920–925. [CrossRef Medline](#)
- Winterer G, Musso F, Konrad A, Vucurevic G, Stoeter P, Sander T, Gallinat J (2007) Association of attentional network function with exon 5 variations of the *CHRNA4* gene. *Hum Mol Genet* 16:2165–2174. [CrossRef Medline](#)
- Yeo BT, Krienen FM, Eickhoff SB, Yaakub SN, Fox PT, Buckner RL, Asplund CL, Chee MW (2015) Functional specialization and flexibility in human association cortex. *Cereb Cortex* 25:3654–3672. [CrossRef Medline](#)